LU TP 12-14
April 2012

Diffractive gauge bosons production beyond QCD factorisation

R. S. Pasechnik*

Department of Astronomy and Theoretical Physics,
Lund University, SE 223-62 Lund, Sweden

B. Z. Kopeliovich, and I. K. Potashnikova

Departamento de Física Universidad Técnica Federico Santa María; and
Instituto de Estudios Avanzados en Ciencias e Ingeniería; and
Centro Científico-Tecnológico de Valparaíso;
Casilla 110-V, Valparaíso, Chile

Abstract

We discuss single diffractive gauge bosons (γ^*, $W^{\pm}$, Z) production in proton-proton collisions at different (LHC and RHIC) energies within the color dipole approach. The calculations are performed for gauge bosons produced at forward rapidities. The diffractive cross section is predicted as function of fractional momentum and invariant mass of the lepton pair. We found a dramatic breakdown of the diffractive QCD factorisation caused by an interplay of hard and soft interactions. Data from the CDF experiment on diffractive production of W and Z are well explained in a parameter free way.

PACS numbers: 13.87.Ce,14.65.Dw

*Electronic address: Roman.Pasechnik@thep.lu.se

I. INTRODUCTION

The characteristic feature of diffractive processes at high energies is presence of a large rapidity gap between the remnants of the beam and target. The general theoretical framework for such processes was formulated in the pioneering works of Glauber [1], Feinberg and Pomeranchuk [2], Good and Walker [3]. The new *diffractive* state is produced only if different Fock components of the incoming plane wave, which are the eigenstates of interaction, interact differently with the target. As a results in a new combination of the Fock components, which can be projected to a new physical state (e.g. see review on QCD diffraction Ref. [4]).

The main difficulty in the formulation of a theoretical QCD-based framework for diffractive scattering arises from the fact that it is essentially contaminated by soft, nonperturbative interactions. For example, diffractive deep-inelastic scattering (DIS), $\gamma^* p \to Xp$, although it is a higher twist process, is dominated by soft interactions [5]. Within the dipole approach [6] such a process looks like elastic scattering of $\bar{q}q$ dipoles of different sizes, and of higher Fock states containing more partons. Although formally the process $\gamma^* \to X$ is an off-diagonal diffraction, it does not vanish in the limit of unitarity saturation, the so called black disc limit. This happens because the photon distribution functions and hadronic wave functions are not orthogonal. Such a principal difference between diffractive processes in DIS and hadronic collisions is one of the reasons for breakdown of diffractive QCD factorization based e.g. on the Ingelman-Schlein model [7]. In particular the cross section of diffractive production of the W boson was found in the CDF experiment [8, 9] to be six times smaller than was predicted relying on factorization and HERA data [10]. The phenomenological models based on assumptions of the diffractive factorisation, which are widely discussed in the literature (see e.g. Refs. [11, 12]), predict a significant increase of the ratio of the diffractive to inclusive gauge bosons production cross sections with energy. This is supposed to be tested soon at the LHC.

The process under discussion, diffractive abelian radiation of electroweak gauge bosons, is the real off-diagonal diffraction. It vanishes in the black-disc limit, and may be strongly suppressed by the absorptive corrections even being far from the unitarity bound. The suppression caused by the absorptive corrections, also known as the survival probability of a large rapidity gap, is related to the initial and final state interactions. Usually the survival probability is introduced in the diffractive cross section in a probabilistic way and is estimated in oversimplified models, like eikonal, quasi-eikonal, two-channel approximations, etc. The advantage of the dipole approach is the possibility to calculate directly (although in a model-dependent way) the full diffractive amplitude, which contains all the absorption corrections, because it employs the phenomenological dipole cross section fitted to data. Below we explicitly single out from the diffractive amplitude the survival probability amplitude as a factor.

Another source of factorization breaking is the simple observation that diffractive abelian radiation by a quark vanishes in the forward direction (zero momentum transfer to the target) [13]. Indeed, the Fock components of the quark with or without the abelian boson (γ^*, Z, W, Higgs boson) interact with the same total cross sections, because only the quark interacts strongly. Therefore, after integration of the amplitude over impact parameter the Fock state decomposition of the projectile remains unchanged, and only elastic qp scattering is possible. Notice that nonabelian radiation (gluons) does not expose this property, because the Fock components $|q\rangle$ and $|q\,g\rangle$, although have the same color, interact differently [13, 14].

In the case of pp collisions the directions of propagation of the proton and its quarks do not coincide. Already this is sufficient to get a nonvanishing diffractive abelian radiation in forward scattering. Moreover, interaction with the spectator partons opens new possibilities for diffractive scattering, namely the color exchange in interaction of one projectile parton, can be compensated (neutralized) by interaction of another projectile parton. It was found in Refs. [15, 16] that this contribution leads to a dominant contribution to the diffractive abelian radiation in the forward direction. This mechanism, leading to a dramatic violation of diffractive QCD factorisation, is under consideration in the present paper. The breakdown of the diffractive (Ingelman-Schlein) QCD factorisation is a result of the interplay between the soft and hard interactions, which considerably affects the corresponding observables [15]. Recently, such an effect has been analyzed in the diffractive Drell-Yan process [15, 16], and here we extend our study of this interesting phenomenon to a more general case – the diffractive gauge boson production.

II. DIFFRACTIVE GAUGE BOSONS PRODUCTION AMPLITUDE

Consider first the general formalism for diffractive radiation of the electroweak gauge bosons, γ^*, Z^0, $W^\pm$, within the color dipole approach. Let us start with consideration of the distribution functions for the Fock states contributing to heavy gauge bosons radiation by a quark (valence or sea) in the projectile proton.

A. Gauge bosons radiation by a quark

The $q_f \to q_f\gamma^*$ transition amplitude is given by the vector $\gamma^* q$ coupling only, i.e.

$$T(q_f \to q_f\gamma^*) = -ieZ_q\varepsilon^\mu_{\lambda_{\gamma^*}}\bar{u}_f\gamma_\mu u_f\,, \tag{2.1}$$

where Z_f is the quark charge, $\bar{u}_f$ and u_f are spinors for the quark of the flavour f in the final and initial states, respectively.

The couplings of Z^0 and $W^\pm$ bosons to quarks contain both vector and axial-vector parts. The $q_f \to q_f Z^0$ transition amplitude is given by

$$T(q_f \to q_f Z^0) = \frac{-ie}{\sin\,2\theta_W}\,\varepsilon^\mu_{\lambda_Z}\bar{u}_f[g^Z_{v,f}\gamma_\mu - g^Z_{a,f}\gamma_\mu\gamma_5]u_f, \tag{2.2}$$

while the $q_f \to q_{f'}W^\pm$ amplitudes read,

$$T(q_{f_u} \to q_{f_d}W^+) = \frac{-ie}{2\sqrt{2}\sin\theta_W}\,V_{f_uf_d}\,\varepsilon^\mu_{\lambda_W}\bar{u}_{f_u}[g^W_{v,f}\gamma_\mu - g^W_{a,f}\gamma_\mu\gamma_5]u_{f_d}, \tag{2.3}$$

$$T(q_{f_d} \to q_{f_u}W^-) = \frac{-ie}{2\sqrt{2}\sin\theta_W}\,V_{f_df_u}\,\varepsilon^\mu_{\lambda_W}\bar{u}_{f_d}[g^W_{v,f}\gamma_\mu - g^W_{a,f}\gamma_\mu\gamma_5]u_{f_u},$$

for the *up* ($f_u = u, c, t$) and *down* ($f_d = d, s, b$) quarks, respectively. Here, $V_{f_uf_d}$ is the CKM matrix element corresponding to $f_u \to f_d$ transition, and θ_W is the Weinberg angle. The weak mixing parameter, $\sin^2\theta_W$, is related at the tree level to G_F, M_Z and α_{em} by $\sin^2\theta_W = 4\pi\alpha_{em}/\sqrt{2}G_FM_Z^2$ (we adopt here $\alpha_{em}(m_Z) \simeq 1/127.934$). The vector couplings at the tree level are

$$g^Z_{v,f_u} = \frac{1}{2} - \frac{4}{3}\sin^2\theta_W, \qquad g^Z_{v,f_d} = -\frac{1}{2} + \frac{2}{3}\sin^2\theta_W, \qquad g^W_{v,f} = 1\,; \tag{2.4}$$

whereas axial-vector couplings are

$$g^Z_{a,f_u} = \frac{1}{2}, \qquad g^Z_{a,f_d} = -\frac{1}{2}\,, \qquad g^W_{a,f} = 1\,. \tag{2.5}$$

Heavy gauge boson polarization vectors describing transverse (T), $\lambda_G = \pm 1$, and longitudinal (L), $\lambda_G = 0$, polarization states are defined in light-cone coordinates[1] as

$$\varepsilon_{\lambda=\pm} = (0,\, 0,\, \vec{\varepsilon}_{\lambda=\pm}), \qquad \vec{\varepsilon}_{\lambda=\pm} = \mp\frac{1}{\sqrt{2}}(1,\, \pm i), \tag{2.6}$$

$$\varepsilon_{\lambda=0} = \left(\frac{q^+}{M},\, -\frac{M}{q^+},\, \vec{0}\right). \tag{2.7}$$

Note that we work in the physical (unitary) gauge. The calculations are performed in the high energy limit, i.e. in the limit where q^+ is much larger than all other scales.

Let us start with the radiation of a heavy gauge boson by a quark interacting with a proton target. We assume that the longitudinal momentum of the projectile is not changed significantly by the soft interaction at high energies. In the high energy limit the corresponding s and u-channel amplitudes of the gauge boson bremsstrahlung in the quark-target scattering can be written as follows (cf. diffractive DY amplitude in Ref. [16]),

$$\begin{aligned}
\mathcal{M}_s &\simeq -i\sqrt{4\pi}\mathcal{C}^G_q\,\alpha(1-\alpha)\,\varepsilon^\mu_\lambda \sum_\sigma \frac{\bar{u}_{\sigma_2}(p_2)[g^G_{v,f}\gamma_\mu - g^G_{a,f}\gamma_\mu\gamma_5]u_\sigma(p_2+q)}{\alpha^2 l^2_\perp + \eta^2}\,\mathcal{A}_{\sigma\sigma_1}(k_\perp),\\
\mathcal{M}_u &\simeq i\sqrt{4\pi}\mathcal{C}^G_q\,\alpha\,\varepsilon^\mu_\lambda \sum_\sigma \frac{\bar{u}_\sigma(p_1-q)[g^G_{v,f}\gamma_\mu - g^G_{a,f}\gamma_\mu\gamma_5]u_{\sigma_1}(p_1)}{\alpha^2(\vec{l}_\perp + \vec{k}_\perp)^2 + \eta^2}\,\mathcal{A}_{\sigma\sigma_2}(k_\perp),
\end{aligned} \tag{2.8}$$

where $G = \gamma$, $W^\pm$, Z is the gauge boson under consideration; $\eta^2 = (1-\alpha)M^2 + \alpha^2 m_q^2$; α is the fractional light-cone momentum carried by the gauge boson, which has invariant mass M. The vector (v) and axial-vector (a) couplings $g^{Z,W}_{v/a,f}$ are defined in Eqs. (2.4) and (2.5), whereas our notations imply $g^\gamma_{v,f} = 1$ and $g^\gamma_{a,f} = 0$; $\sigma_{1,2}$ are the helicities of initial and final quarks, respectively; $\vec{k}_\perp = \vec{p}_{2\perp} - \vec{p}_{1\perp} + \vec{q}_\perp$ is the transverse momentum of the exchanged gluon; and $\vec{l}_\perp = \vec{p}_{2\perp} - (1-\alpha)\vec{q}_\perp/\alpha$ is the transverse momentum of the final quark in the frame, where z-axis is parallel to the gauge boson momentum. The amplitude $\mathcal{A}$ for scattering of the quark on the nucleon in the target rest frame has the following approximate form, [23]

$$\mathcal{A}_{\sigma\sigma_1}(\vec{k}_\perp) \simeq 2p^0_1\delta_{\sigma\sigma_1}\mathcal{V}_q(\vec{k}_\perp), \qquad \mathcal{A}_{\sigma\sigma_2}(\vec{k}_\perp) \simeq 2p^0_2\delta_{\sigma\sigma_2}\mathcal{V}_q(\vec{k}_\perp)\,,$$

where the factorized universal amplitude $\mathcal{V}_q(\vec{k}_\perp)$ does not depend on energy and helicity state of the quark. The coupling factor $\mathcal{C}^G_f$, $f = q, l$, introduced in Eq. (2.8), is defined for $G = \gamma^*$, Z^0 and $W^\pm$ bosons, respectively, as

$$\mathcal{C}^\gamma_f = \sqrt{\alpha_{em}}Z_f, \qquad \mathcal{C}^Z_f = \frac{\sqrt{\alpha_{em}}}{\sin 2\theta_W}, \qquad \mathcal{C}^{W^+}_f = \frac{\sqrt{\alpha_{em}}}{2\sqrt{2}\sin\theta_W}V_{f_u f_d}, \qquad \mathcal{C}^{W^-}_f = \frac{\sqrt{\alpha_{em}}}{2\sqrt{2}\sin\theta_W}V_{f_d f_u}\,,$$

[1] As usual, the light-cone 4-vector p is defined as $p = (p^+,\, p^-,\, \vec{p})$, where $p^\pm = p^0 \pm p^z$.

where $\alpha_{em} = e^2/(4\pi) = 1/137$ is the electromagnetic coupling constant. In the case of gauge boson couplings to leptons we should substitute $V_{f_u f_d} = V_{f_d f_u} = 1$.

Eventually, we can switch to impact parameter space performing the Fourier transformation over $\vec{l}_\perp$ and $\vec{k}_\perp$, and write down the total amplitude M_q for gauge boson radiation in quark-proton scattering as follows,

$$M_q^\mu(\vec{b},\vec{r}) = -2ip_1^0\sqrt{4\pi}\,\frac{\sqrt{1-\alpha}}{\alpha^2}\,\Psi^\mu_{V-A}(\vec{r},\alpha,M)\cdot\Big[V_q(\vec{b}) - V_q(\vec{b}+\alpha\vec{r})\Big],$$
$$V_q(\vec{b}) = \int\frac{d^2k_\perp}{(2\pi)^2}e^{-i\vec{k}_\perp\cdot\vec{b}}\mathcal{V}_q(\vec{k}_\perp),\quad \Psi^{Z,W}_{V-A}(\vec{r},\alpha,M) = \Psi^{Z,W}_{V}(\vec{r},\alpha,M) - \Psi^{Z,W}_{A}(\vec{r},\alpha,M)\,,$$

where $\alpha\vec{r}$ is the transverse separation between the initial and final quarks; $\Psi^\mu_{V/A}(\vec{r},\alpha,M)$ are the light-cone distribution functions of the vector $q\to Vq$ and axial-vector $q\to Aq$ transitions in the mixed representation defined as,

$$\Psi^\mu_V(\vec{r},\alpha,M) = \mathcal{C}_q^G g^G_{v,q}\,\alpha^3\sqrt{1-\alpha}\int\frac{d^2l_\perp}{(2\pi)^2}e^{-i\vec{l}_\perp\cdot\alpha\vec{r}}\,\frac{\bar{u}_{\sigma_2}(p_f)\gamma^\mu u_\sigma(p_2+q)}{\alpha^2 l_\perp^2+\eta^2},$$
$$\Psi^\mu_A(\vec{r},\alpha,M) = \mathcal{C}_q^G g^G_{a,q}\,\alpha^3\sqrt{1-\alpha}\int\frac{d^2l_\perp}{(2\pi)^2}e^{-i\vec{l}_\perp\cdot\alpha\vec{r}}\,\frac{\bar{u}_{\sigma_2}(p_2)\gamma^\mu\gamma_5 u_\sigma(p_2+q)}{\alpha^2 l_\perp^2+\eta^2}\,.$$

For an unpolarized initial quark the interference terms between the vector and axial-vector wave functions cancel each other, i.e.

$$\sum_{\sigma_1,\sigma_2}\Psi^\lambda_{V-A}(\alpha,\vec{\rho}_1)\Psi^{\lambda *}_{V-A}(\alpha,\vec{\rho}_2) = \Psi^\lambda_V(\alpha,\vec{\rho}_1)\Psi^{\lambda *}_V(\alpha,\vec{\rho}_2) + \Psi^\lambda_A(\alpha,\vec{\rho}_1)\Psi^{\lambda *}_A(\alpha,\vec{\rho}_2)\,. \tag{2.9}$$

The bilinear combinations of the vector V and axial-vector A light-cone distribution functions, corresponding to radiation of longitudinally ($\lambda=0$) and transversely ($\lambda=\pm1$) polarized gauge bosons have the form[2],

$$\Psi^T_V(\alpha,\vec{\rho}_1)\Psi^{T*}_V(\alpha,\vec{\rho}_2) = \sum_{\lambda=\pm1}\frac{1}{2}\sum_{\sigma_1,\sigma_2}\epsilon^*_\mu(\lambda)\Psi^\mu_V(\alpha,\vec{\rho}_1)\epsilon_\nu(\lambda)\Psi^{\nu *}_V(\alpha,\vec{\rho}_2) \tag{2.10}$$
$$= \frac{\mathcal{C}_q^2(g^G_{v,q})^2}{2\pi^2}\Bigg\{m_q^2\alpha^4\mathrm{K}_0\left(\eta\rho_1\right)\mathrm{K}_0\left(\eta\rho_2\right) + \left[1+(1-\alpha)^2\right]\eta^2\frac{\vec{\rho}_1\cdot\vec{\rho}_2}{\rho_1\rho_2}\mathrm{K}_1\left(\eta\rho_1\right)\mathrm{K}_1\left(\eta\rho_2\right)\Bigg\},$$
$$\Psi^L_V(\alpha,\vec{\rho}_1)\Psi^{L*}_V(\alpha,\vec{\rho}_2) = \frac{1}{2}\sum_{\sigma_1,\sigma_2}\epsilon^*_\mu(\lambda=0)\Psi^\mu_V(\alpha,\vec{\rho}_1)\epsilon_\nu(\lambda=0)\Psi^{\nu *}_V(\alpha,\vec{\rho}_2)$$
$$= \frac{\mathcal{C}_q^2(g^G_{v,q})^2}{\pi^2}M^2\left(1-\alpha\right)^2\mathrm{K}_0\left(\eta\rho_1\right)\mathrm{K}_0\left(\eta\rho_2\right)\,.$$

$$\Psi^T_A(\alpha,\vec{\rho}_1)\Psi^{T*}_A(\alpha,\vec{\rho}_2) = \tag{2.11}$$
$$= \frac{\mathcal{C}_q^2(g^G_{a,q})^2}{2\pi^2}\Bigg\{m_q^2\alpha^2(2-\alpha)^2\mathrm{K}_0\left(\eta\rho_1\right)\mathrm{K}_0\left(\eta\rho_2\right) + \left[1+(1-\alpha)^2\right]\eta^2\frac{\vec{\rho}_1\cdot\vec{\rho}_2}{\rho_1\rho_2}\mathrm{K}_1\left(\eta\rho_1\right)\mathrm{K}_1\left(\eta\rho_2\right)\Bigg\},$$
$$\Psi^L_A(\alpha,\vec{\rho}_1)\Psi^{L*}_A(\alpha,\vec{\rho}_2) = \frac{\mathcal{C}_q^2(g^G_{a,q})^2}{\pi^2}\frac{\eta^2}{M^2}\Bigg\{\eta^2\mathrm{K}_0\left(\eta\rho_1\right)\mathrm{K}_0\left(\eta\rho_2\right) + \alpha^2 m_q^2\frac{\vec{\rho}_1\cdot\vec{\rho}_2}{\rho_1\rho_2}\mathrm{K}_1\left(\eta\rho_1\right)\mathrm{K}_1\left(\eta\rho_2\right)\Bigg\}.$$

where the averaging over helicity of the initial quark is performed.

[2] In the case of a heavy photon γ^* bremsstrahlung by a quark such formulae were derived in Refs. [22–24].

B. Forward diffractive radiation from a dipole

The amplitude of diffractive gauge boson radiation by a quark-antiquark dipole does not vanish in forward direction, unlike the radiation by a single quark [13, 15]. This can be understood as follows. When a quark fluctuates into a state $|qG\rangle$ containing the gauge boson G, with the transverse quark-boson separation $\vec{r}$, the quark gets a transverse shift $\Delta\vec{r} = \alpha\vec{r}$. Nevertheless, both Fock states $|q\rangle$ and $|qG\rangle$, interact with the target with the same total cross section, this is why G is not produced diffractively in the forward direction. The situation changes if the boson is radiated diffractively by a dipole. Then the quark dipoles with or without a gauge boson have different sizes and interact with the target differently. So the amplitude of the diffractive gauge boson radiation from the $q\bar{q}$ dipole is proportional to the difference between elastic amplitudes of the two Fock components, $|q\bar{q}\rangle$ and $|q\bar{q}G\rangle$[15], i.e.

$$M_{\bar{q}q}(\vec{b},\vec{r}_p,\vec{r},\alpha) = -2ip_1^0\sqrt{4\pi}\,\frac{\sqrt{1-\alpha}}{\alpha^2}\,\Psi^{\mu}_{\gamma^* q}(\alpha,\vec{r})\,\Big[2\mathrm{Im}\,f_{el}(\vec{b},\vec{r_p}) - 2\mathrm{Im}\,f_{el}(\vec{b},\vec{r}_p+\alpha\vec{r})\Big] \quad (2.12)$$

where $\vec{r}_p$ is the transverse separation of the $q\bar{q}$ dipole. The partial elastic dipole-proton amplitude is normalized to the dipole cross section, which is parameterized by the following simple ansatz [32],

$$\sigma_{\bar{q}q}(r_p,x) = \int d^2b\,2\,\mathrm{Im}f_{el}(\vec{b},\vec{r}_p) = \sigma_0(1-e^{-r_p^2/R_0^2(x)}) \quad (2.13)$$

This saturated form, although is oversimplified (compare with [33]), is rather successful in description of experimental HERA data with a reasonable accuracy. We rely on this parametrization in what follows, and the parameters σ_0 and $R_0(x)$, as well as the explicit form of the amplitude $f_{el}(\vec{b},\vec{r})$, will be specified later.

The diffractive amplitude (2.12), thus, occurs to be sensitive to the large transverse separations between the projectile quarks in the incoming proton. These distances are controlled by a nonperturbative scale, which is one of the reasons for the breakdown of diffractive QCD factorisation in the diffractive gauge bosons production (for more details, see Refs. [15, 16]).

III. SINGLE DIFFRACTIVE CROSS SECTION

The differential cross section for the single diffractive di-lepton ($l\bar{l}$ pair in the case of γ^*, Z and $l\nu_l$ pair in the case of $W^{\pm}$) production in the target rest frame can be written in terms of the gauge boson production cross section at a given invariant mass of the di-lepton M. Integrating the cross section over the solid angle of the lepton pair and the boson transverse momentum $\vec{q}_\perp$ we get for the diffractive Drell-Yan cross section [16],

$$\frac{d^6\sigma_{L,T}(pp\to pl\bar{l}X)}{d^2q_\perp dx_1\,dM^2\,d^2\delta_\perp} = \frac{\alpha_{em}}{3\pi M^2}\,\frac{d^5\sigma_{L,T}(pp\to p\gamma^*X)}{d^2q_\perp dx_1\,d^2\delta_\perp}\,, \quad (3.1)$$

where x_1 is the fractional light-cone momentum of the di-lepton, $\vec{\delta}_\perp$ is the transverse momentum of the recoil proton, and $\vec{q}_\perp$ is the transverse momentum of the outgoing photon (or di-lepton). Compared to our previous study, here we are going to look at the $q_\perp$-dependence

of the diffractive DY cross section in a much wider range of di-lepton invariant masses accessible at the LHC.

In the case of the diffractive production of $G = Z^0$, $W^\pm$ bosons, it is convenient to employ the simple and phenomenologically successful model for the invariant mass distribution in the decay of an unstable particle (for details, see e.g. Refs. [21]) and to present the differential cross section in the factorized form,

$$\frac{d^4\sigma_{L,T}(pp \to p(G^* \to l\bar{l},\, l\bar{\nu}_l)X)}{d^2q_\perp dx_1\, dM^2\, d^2\delta_\perp} = \mathrm{Br}(G \to l\bar{l},\, l\nu_l)\, \rho_G(M)\, \frac{d^3\sigma_{L,T}(pp \to pG^*X)}{d^2q_\perp dx_1\, d^2\delta_\perp}\,, \quad (3.2)$$

where $\mathrm{Br}(Z^0 \to \sum_{l=e,\mu,\tau} l\bar{l}) \simeq 0.101$ and $\mathrm{Br}(W^\pm \to \sum_{l=e,\mu,\tau} l\nu_l) \simeq 0.326$ [19] are the leptonic branching ratios of Z^0 and $W^\pm$ bosons, and $\rho_G(M)$ is the invariant mass distribution of the dileptons from the decay of the gauge boson G,

$$\rho_G(M) = \frac{1}{\pi}\frac{M\,\Gamma_G(M)}{(M^2 - m_G^2)^2 + [M\,\Gamma_G(M)]^2}\,, \quad \Gamma_G(M)/M \ll 1\,. \quad (3.3)$$

Here, m_G is the fixed on-shell boson mass and $\Gamma_G(M)$ is its total decay width defined in the standard way by substitution $m_G \to M$, i.e.

$$\Gamma_W(M) \simeq \frac{3\alpha_{em}\, M}{4\sin^2\theta_W}\,, \qquad \Gamma_Z(M) \simeq \frac{\alpha_{em} M}{6\sin^2 2\theta_W}\left[\frac{160}{3}\sin^4\theta_W - 40\sin^2\theta_W + 21\right] \quad (3.4)$$

Let us assume that the gauge boson is emitted by the quark q_1. As a result of the hard emission the quark position in the impact parameters, being initially $\vec{r}_1$, gets shifted to $\vec{r}_1 + \alpha\vec{r}$. Applying the completeness relation to the wave function of the proton remnant in the final state

$$\sum_f \Psi_f(\vec{r}_1 + \alpha\vec{r}, \vec{r}_2, \vec{r}_3; \{x_q^{1,2,\cdots}\}, \{x_g^{1,2,\cdots}\})\Psi_f^*(\vec{r}\,'_1 + \alpha\vec{r}\,', \vec{r}\,'_2, \vec{r}\,'_3; \{x'^{1,2,\cdots}_q\}, \{x'^{1,2,\cdots}_g\})$$
$$= \delta\big(\vec{r}_1 - \vec{r}\,'_1 + \alpha(\vec{r} - \vec{r}\,')\big)\delta(\vec{r}_2 - \vec{r}\,'_2)\delta(\vec{r}_3 - \vec{r}\,'_3)\prod_j \delta(x^j_{q/g} - x'^j_{q/g}), \quad (3.5)$$

where $\vec{r}_i$, $x^i_{q/g}$ are the transverse coordinates and fractional light-cone momenta of the valence/sea quarks and gluons, we get the diffractive G^* production cross section in the following form [15, 16]

$$\frac{d^5\sigma_{\lambda_G}(pp \to pG^*X)}{d^2q_\perp dx_1\, d^2\delta_\perp} = \frac{1}{(2\pi)^2}\frac{1}{64\pi^2}\frac{1}{x_1}\sum_{q=val,\,sea}\int d^2r_1 d^2r_2 d^2r_3\, d^2r d^2r'\, d^2b d^2b'\, dx_q \prod_i dx_q^i dx_g^i$$
$$\times \Psi^{\lambda_G}_{V-A}(\vec{r}, \alpha, M)\Psi^{\lambda_G *}_{V-A}(\vec{r}\,', \alpha, M)\,|\Psi_i(\vec{r}_1, \vec{r}_2, \vec{r}_3; x_q, \{x_q^{2,3,\cdots}\}, \{x_g^{2,3,\cdots}\})|^2$$
$$\times \Delta(\vec{r}_1, \vec{r}_2, \vec{r}_3; \vec{b}; \vec{r}, \alpha)\Delta(\vec{r}_1, \vec{r}_2, \vec{r}_3; \vec{b}\,'; \vec{r}\,', \alpha)\, e^{i\vec{\delta}_\perp\cdot(\vec{b} - \vec{b}\,')}\, e^{i\vec{l}_\perp\cdot\alpha(\vec{r} - \vec{r}\,')} \quad (3.6)$$

where Ψ_i is the proton wave function, the summation is performed over all valence/sea quarks and gluons in the proton, and the light-cone fraction of the quark emitting the gauge boson $x_q^1 \equiv x_q$ is fixed by the external phase space variables x_1 and α due to the momentum conservation, namely,

$$x_q = \frac{x_1}{\alpha}\,, \qquad x_1 = \frac{q^+}{P_1^+} \quad (3.7)$$

where P_1 is the 4-momentum of the projectile proton, q is the 4-momentum of the produced gauge boson, and

$$\begin{aligned}\Delta \;=\; & -2\mathrm{Im}\, f_{el}(\vec{b},\vec{r}_1-\vec{r}_2)+2\mathrm{Im}\, f_{el}(\vec{b},\vec{r}_1-\vec{r}_2+\alpha\vec{r}) \\ & -2\mathrm{Im}\, f_{el}(\vec{b},\vec{r}_1-\vec{r}_3)+2\mathrm{Im}\, f_{el}(\vec{b},\vec{r}_1-\vec{r}_3+\alpha\vec{r})\,, \end{aligned} \tag{3.8}$$

is the properly normalized diffractive amplitude, where $f_{el}(\vec{b},\vec{r}_1-\vec{r}_2)$ is the partial elastic amplitude for dipole of transverse size r colliding with a proton at impact parameter b to be specified below. As expected, the diffractive amplitude Δ is proportional to the difference between elastic amplitudes for the dipoles of slightly different sizes. This difference is suppressed by absorptive corrections, the effect sometimes called survival probability of large rapidity gaps.

The amplitude Eq. (3.8) is the full expression, which includes by default the effect of absorption and does not need any extra survival probability factor[3]. This can be illustrated on a simple example of elastic dipole scattering off a potential. The dipole elastic amplitude has the eikonal form,

$$\mathrm{Im}\, f_{el}(\vec{b},\vec{r}_1-\vec{r}_2)=1-\exp\big[i\chi(\vec{r}_1)-i\chi(\vec{r}_2)\big], \tag{3.9}$$

where

$$\chi(b)=-\int\limits_{-\infty}^{\infty} dz\, V(\vec{b},z), \tag{3.10}$$

and $V(\vec{b},z)$ is the potential, which depends on the impact parameter and longitudinal coordinate, and is nearly imaginary at high energies. The difference between elastic amplitudes with a shifted quark position, which enters the diffractive amplitude, reads,

$$\mathrm{Im}\, f_{el}(\vec{b},\vec{r}_1-\vec{r}_2+\alpha\vec{r})-\mathrm{Im}\, f_{el}(\vec{b},\vec{r}_1-\vec{r}_2)=\exp\big[i\chi(\vec{r}_1)-i\chi(\vec{r}_2)\big]\,\exp\big[i\alpha\,\vec{r}\cdot\vec{\nabla}\chi(\vec{r}_1)\big]. \tag{3.11}$$

The first factor $\exp\big[i\chi(\vec{r}_1)-i\chi(\vec{r}_2)\big]$ is exactly the survival probability amplitude, which vanishes in the black disc limit, as it should be. This proves that the cross section Eq. (3.6) includes the effect of absorption. Notice that usually the survival probability factor is introduced into the diffractive cross section probabilistically, while in Eq. (3.6) it is treated quantum-mechanically, at the amplitude level.

All the elastic amplitudes in Eq. (3.8) implicitly depend on energy. They cannot be calculated reliably, but but are known from phenomenology. Since large dipole sizes $|\vec{r}_i-\vec{r}_j|\sim b\sim R_p$, $i\neq j$ (R_p is the mean proton size) are important in Eq. (3.8), the Bjorken variable x is ill defined, and the collisions energy is a more appropriate variable. A parametrization of the dipole cross section as function of s was proposed and fitted to data in Ref. [13], and the corresponding partial dipole amplitude is given by [25–27]

$$\begin{aligned}\mathrm{Im} f_{el}(\vec{b},\vec{r}_p,s,x_q)=\frac{\sigma_0(s)}{8\pi\mathcal{B}(s)}\Bigg\{ & \exp\left[-\frac{[\vec{b}+\vec{r}_p(1-x_q)]^2}{2\mathcal{B}(s)}\right]+\exp\left[-\frac{[\vec{b}+\vec{r}_p x_q]^2}{2\mathcal{B}(s)}\right] \\ & -2\exp\left[-\frac{r_p^2}{R_0^2(s)}-\frac{[\vec{b}+\vec{r}_p(1/2-x_q)]^2}{2\mathcal{B}(s)}\right]\Bigg\},\quad \mathcal{B}(s)=R_N^2(s)+R_0^2(s)/8\,, \end{aligned} \tag{3.12}$$

[3] Such a statement has already been made in a similar analysis of the diffractive heavy flavor production performed in Ref. [14] and in our previous work on diffractive DY study [16].

where x_q is the quark longitudinal quark fraction in the dipole defined in Eq. (3.7), and

$$R_0(s) = 0.88\,\mathrm{fm}\,(s_0/s)^{0.14}\,, \quad R_N^2(s) = B_{el}^{\pi p}(s) - \frac{1}{4}R_0^2(s) - \frac{1}{3}\langle r_{ch}^2\rangle_\pi\,,$$
$$\sigma_0(s) = \sigma_{tot}^{\pi p}(s)\Big(1 + \frac{3R_0^2(s)}{8\langle r_{ch}^2\rangle_\pi}\Big)\,. \tag{3.13}$$

Here, the pion-proton total cross section is parameterized as [29] $\sigma_{tot}^{\pi p}(s) = 23.6(s/s_0)^{0.08}$ mb, $s_0 = 1000\,\mathrm{GeV}^2$, the mean pion radius squared is [31] $\langle r_{ch}^2\rangle_\pi = 0.44$ fm^2, and the Regge parametrization of the elastic slope $B_{el}^{\pi p}(s) = B_0 + 2\alpha'_{I\!P}\ln(s/\mu^2)$, with $B_0 = 6\,\mathrm{GeV}^{-2}$, $\alpha'_{I\!P} = 0.25\,\mathrm{GeV}^{-2}$, and $\mu^2 = 1\,\mathrm{GeV}^2$ can be used. We employ the s-dependent parametrization (3.12) in what follows, because diffraction is essentially controlled by soft interactions.

Finally, we parameterize the proton wave function assuming the symmetric Gaussian shape for the spacial valence quark distributions in the proton, as

$$|\Psi_i(\vec{r}_1,\vec{r}_2,\vec{r}_3;x_q,\{x_q^{2,3,\cdots}\},\{x_g^{2,3,\cdots}\})|^2 \;=\; \frac{3a^2}{\pi^2}e^{-a(r_1^2+r_2^2+r_3^2)}\rho(x_q,\{x_q^{2,3,\cdots}\},\{x_g^{2,3,\cdots}\})$$
$$\times\;\delta(\vec{r}_1+\vec{r}_2+\vec{r}_3)\delta(1-x_q-\sum_j x_{q/g}^j), \tag{3.14}$$

where sum is taken over all valence/sea quarks and gluons not participating in the hard interaction, x_q is defined in Eq. (3.7), $a = \langle r_{ch}^2\rangle^{-1}$ is the inverse proton mean charge radius squared; ρ is the valence quark distribution function in the proton. Notice that this distribution has a low scale, so the valence quark carry the whole momentum of the proton, while gluons and the sea are included in the constituent valence quarks. The Gottfried sum rule based on this assumption is know to be broken [30], but we neglect the related $\sim 20\%$ correction.

Integrating over the fractional momenta of all partons not participating in the hard interaction we arrive at the single valence quark distribution in the proton, probed by the hard process – radiation of a heavy gauge boson,

$$\int\prod_i dx_q^i dx_g^i\,\delta(1-x_q-\sum_j x_{q/g}^j)\rho(x_q,\{x_q^{2,3,\cdots}\},\{x_g^{2,3,\cdots}\}) = \rho_q(x_q)\,, \tag{3.15}$$

where q denotes the quark flavor emitting the gauge boson G with the fraction x_q given by Eq. (3.7). In the case of diffractive Drell-Yan reaction [16], generalization of the three-body proton wave function (3.14) including different quark and antiquark flavors leads to the proton structure function as,

$$\sum_q Z_q^2[\rho_q(x_q) + \rho_{\bar{q}}(x_q)] = \frac{1}{x_q}F_2(x_q)\,. \tag{3.16}$$

However, in the case of diffractive W and Z production the coupling factor $\mathcal{C}_q^G g_{v/a,q}^G$ varies for different (valence/sea) quark species in the proton, so one has to deal with the original quark densities. Similar to the diffractive DY case, in actual numerical calculations below, when summing up the contributions of different quark flavors, we will generalize the above approach including the sea quark and antiquark densities in the proton at the hard scale imposed by the mass of the gauge boson. Also, the interference terms between amplitudes corresponding to gauge boson radiated by different valence quarks separated by large transverse distances in the proton are strongly suppressed in the hard limit $r \ll R_0(s)$, and are neglected.

IV. SINGLE DIFFRACTIVE CROSS SECTION IN THE FORWARD LIMIT

Since the fluctuation of the dipole size caused by the hard vector boson production, $\alpha r \sim \alpha/(1-\alpha)M$, is typically much smaller than the (semi)soft hadron scale $|\vec{r}_i - \vec{r}_j| \sim b \sim R_p$, $i \neq j$, one can derive an approximate analytical formulae for the diffractive cross section (3.6),

$$\mathrm{Im}\, f_{el}(\vec{b}, \vec{R}_{ij} + \alpha\vec{r}) - \mathrm{Im}\, f_{el}(\vec{b}, \vec{R}_{ij}) \simeq \frac{\partial \mathrm{Im}\, f_{el}(\vec{b}, \vec{R}_{ij})}{\partial \vec{R}_{ij}}\, \alpha\vec{r}, \tag{4.1}$$

where $\vec{R}_{ij} = \vec{r}_i - \vec{r}_j$. For the sake of convenience, let us transform the integrals in Eq. (3.6) by introducing new variables $\vec{r}_2 \to \vec{R}_{12}$ and $\vec{r}_3 \to \vec{R}_{13}$, so that,

$$\int d^2r_1 d^2r_2 d^2r_3\, e^{-a(r_1^2+r_2^2+r_3^2)} \delta(\vec{r}_1 + \vec{r}_2 + \vec{r}_3) = \frac{1}{9}\int d^2R_{12} d^2R_{13} e^{-\frac{2a}{3}(R_{12}^2 + R_{13}^2 + \vec{R}_{12}\vec{R}_{13})}. \tag{4.2}$$

Since in the forward limit $\delta_\perp \to 0$ the b-dependence comes only into the partial dipole amplitude f_{el} defined in Eq. (3.12), it can be easily integrated [15],

$$\int d^2b\, \frac{\partial \mathrm{Im}\, f_{el}(\vec{b}, \vec{R}_{ij})}{\partial \vec{R}_{ij}} = \frac{\sigma_0(s)}{R_0^2(s)}\, \vec{R}_{ij}\, e^{-R_{ij}^2/R_0^2(s)}\,, \tag{4.3}$$

with the energy dependent parameters defined after Eq. (3.12).

We see that the amplitude of diffractive gauge boson emission in the dipole-target scattering (2.12) integrated over $\vec{b}$,

$$\int d^2b\, M_{qq}(\vec{b}, \vec{R}_{ij}, \vec{r}, \alpha) \propto \alpha \frac{\sigma_0(s)}{R_0^2(s)}\, (\vec{r}\cdot\vec{R}_{ij})\, e^{-R_{ij}^2/R_0^2(s)}, \tag{4.4}$$

is proportional to the product of the hard scale $r \sim 1/(1-\alpha)M$ and the soft hadronic scale $R_{ij} \sim R_0 \sim 1/\Lambda_{QCD}$. This means that the single diffractive cross section depends on the hard scale as $\sigma_{sd} \sim r^2 \sim 1/M^2$.

It is well-known that the cross section of diffractive Deep-Inelastic-Scattering (DDIS) $\sigma_{\mathrm{DDIS}} \sim r^4$ is dominated essentially by soft fluctuations at large r (for more details, see e.g. Ref. [5]), as correctly predicted by the diffractive (Ingelman-Schlein) QCD factorisation. This happens since the end-point $q\bar{q}$ dipole fluctuations, driving the cross section at $\alpha \to 0$ or 1, have no hard scale dependence for light quarks $m_q \ll Q^2$. In this case, the Q^2-dependence comes only into their weight as $\sim 1/Q^2$, even though it is of the higher twist nature.

In opposite, the single diffractive gauge bosons production cross section behaves as $\sim \vec{r}\cdot\vec{R}$, soft and hard fluctuations contribute in this process on the same footing, and their interplay does not depend on the hard scale, similar to the inclusive gauge bosons production. Hence, the forward diffractive abelian radiation turns out to be of the leading twist nature, and the diffractive-to-inclusive production cross sections ratio can depend on the hard scale only weakly through the x-dependence of the saturation scale, or more precisely $R_0(x_2)$, and can only increase (see below).

However, if one uses the conventional diffractive factorisation scheme [7] the single diffractive cross section, similarly to the DDIS process, one does not find any soft-hard interplay

as observed above, and the cross section turns out to behave as $\sim r^4$, providing the higher twist nature of the single diffractive process. Correspondingly, this strongly affects the M^2-dependence of the diffractive-to-inclusive boson production cross sections ratio, such that it decreases with M^2, as opposite to our observation above.

Therefore, the fundamental interplay between the hard and soft interactions in the forward diffractive Abelian radiation is *the major reason for the diffractive QCD factorisation breaking* leading to quite unusual features of the corresponding observables (for a similar discussion in the diffractive DY, see Refs. [15, 16]). As we have emphasized above, this interplay is absent in the DDIS and in diffractive QCD factorisation-based approaches to the diffractive DY (see e.g. Ref. [11]) leading to the energy and scale dependence of the corresponding cross section which is completely opposite to the one predicted above by the Color Dipole model.

Further, the integrations over $\vec{R}_{12}$ and $\vec{R}_{13}$ can be performed analytically leading to the diffractive cross section (3.6) in the forward limit $\delta_\perp \to 0$,

$$\frac{d^4\sigma_{\lambda_G}(pp\to p\,G^*X)}{d^2q_\perp dx_1\,d\delta_\perp^2}\Big|_{\delta_\perp=0} = \frac{a^2}{24\pi^3}\frac{\sigma_0^2(s)}{R_0^4(s)}\,\frac{1}{A_2}\Big[\frac{2}{(A_2-4A_1)^2}+\frac{A_2^2}{(A_2^2-4A_3^2)^2}\Big]\times \tag{4.5}$$
$$\sum_q\int_{x_1}^1 d\alpha\,\Big[\rho_q\Big(\frac{x_1}{\alpha}\Big)+\rho_{\bar q}\Big(\frac{x_1}{\alpha}\Big)\Big]\int d^2r d^2r'\,(\vec r\cdot\vec r')\,\Psi_{V-A}^{\lambda_G}(\vec r,\alpha,M)\Psi_{V-A}^{\lambda_G*}(\vec r',\alpha,M)\,e^{i\vec q_\perp\cdot(\vec r-\vec r')},$$

where

$$A_1=\frac{2a}{3}+\frac{2}{R_0^2(s)}\,,\qquad A_2=\frac{2a}{3}\,,\qquad A_3=\frac{2a}{3}+\frac{1}{R_0^2(s)}\,. \tag{4.6}$$

Assuming gaussian $\delta_\perp$ dependence of the cross section, the $\delta_\perp$ integrated and forward cross sections are related as,

$$\frac{d\sigma(pp\to p\,G^*X)}{d^2q_\perp dx_1}=\frac{1}{B_{sd}(s)}\frac{d^3\sigma(pp\to p\,G^*X)}{d^2q_\perp dx_1\,d\delta_\perp^2}\Big|_{\delta_\perp=0}. \tag{4.7}$$

The slope of the single-diffractive cross section, $B_{sd}(s)\simeq\langle r_{ch}^2\rangle/3+2\alpha'_{I\!P}\ln(s/s_0)$, is similar to the one measured in diffractive DIS. In the next section we will explicitly derive the diffractive slope from the explicit parameterisation for the partial dipole amplitude (3.12).

Finally, one can explicitly calculate the remaining integrations in the transverse plane over $\vec r$ and $\vec r'$ by means of the following Fourier transforms

$$J_1(q_\perp,\eta)\equiv\int d^2rd^2r'\,(\vec r\cdot\vec r')\,K_0(\eta r)K_0(\eta r')\,e^{i\vec q_\perp\cdot(\vec r-\vec r')}=16\pi^2\frac{q_\perp^2}{(\eta^2+q_\perp^2)^4}\,,$$
$$J_2(q_\perp,\eta)\equiv\int d^2rd^2r'\,\frac{(\vec r\cdot\vec r')^2}{rr'}\,K_1(\eta r)K_1(\eta r')\,e^{i\vec q_\perp\cdot(\vec r-\vec r')}=8\pi^2\frac{\eta^4+q_\perp^4}{\eta^2(\eta^2+q_\perp^2)^4}\,. \tag{4.8}$$

And we arrive at the following expressions for the cross section of transversely and longitudinally polarized gauge boson production, respectively,

$$\frac{d^4\sigma_T(pp\to p\,G^*X)}{d^2q_\perp dx_1}=\frac{1}{B_{sd}(s)}\frac{a^2}{24\pi^3}\frac{\sigma_0^2(s)}{R_0^4(s)}\,\frac{1}{A_2}\Big[\frac{2}{(A_2-4A_1)^2}+\frac{A_2^2}{(A_2^2-4A_3^2)^2}\Big]\times \tag{4.9}$$
$$\sum_q\frac{(\mathcal{C}_q^G)^2}{2\pi^2}\int_{x_1}^1 d\alpha\,\Big[\rho_q\Big(\frac{x_1}{\alpha}\Big)+\rho_{\bar q}\Big(\frac{x_1}{\alpha}\Big)\Big]\Big\{m_q^2\alpha^2\Big[(g_{v,q}^G)^2\alpha^2+(g_{a,q}^G)^2(2-\alpha)^2\Big]J_1+$$
$$\Big[(g_{v,q}^G)^2+(g_{a,q}^G)^2\Big]\,\big[1+(1-\alpha)^2\big]\,\eta^2J_2\Big\}\,;$$

$$\frac{d^4\sigma_L(pp\to p\,G^*X)}{d^2q_\perp dx_1}=\frac{1}{B_{sd}(s)}\frac{a^2}{24\pi^3}\frac{\sigma_0^2(s)}{R_0^4(s)}\,\frac{1}{A_2}\Big[\frac{2}{(A_2-4A_1)^2}+\frac{A_2^2}{(A_2^2-4A_3^2)^2}\Big]\times \quad (4.10)$$
$$\sum_q\frac{(\mathcal{C}_q^G)^2}{\pi^2}\int_{x_1}^1 d\alpha\left[\rho_q\Big(\frac{x_1}{\alpha}\Big)+\rho_{\bar q}\Big(\frac{x_1}{\alpha}\Big)\right]\Big\{\Big[(g_{v,q}^G)^2M^2\,(1-\alpha)^2+(g_{a,q}^G)^2\frac{\eta^4}{M^2}\Big]J_1+$$
$$(g_{a,q}^G)^2\alpha^2m_q^2\frac{\eta^2}{M^2}\,J_2\Big\}\,.$$

These expressions for the differential distributions in the transverse momentum of the produced gauge bosons allow us to perform $\vec{q}_\perp$-integration via the substitution,

$$J_1(q_\perp,\eta)\to I_1(\eta)\equiv\int d^2q_\perp\,J_1(q_\perp,\eta)=\frac{8\pi^3}{3\eta^4}\,,$$
$$J_2(q_\perp,\eta)\to I_2(\eta)\equiv\int d^2q_\perp\,J_2(q_\perp,\eta)=\frac{16\pi^3}{3\eta^4}\,.$$

The left integrations over α and x_1 can be done numerically.

V. DIFFRACTIVE VS INCLUSIVE PRODUCTION OF GAUGE BOSONS

The dipole description of inclusive Gauge boson production can be obtained generalizing what is known for the inclusive Drell-Yan process [22, 24, 28]. The cross section of inclusive production of a virtual gauge boson G^* with mass M and transverse momentum $q_\perp$ has the form,

$$\frac{d^4\sigma_{\lambda_G}(pp\to G^*X)}{d^2q_\perp\,dx_1}=\frac{1}{(2\pi)^2}\sum_q\int_{x_1}^1\frac{d\alpha}{\alpha^2}\left[\rho_q\Big(\frac{x_1}{\alpha}\Big)+\rho_{\bar q}\Big(\frac{x_1}{\alpha}\Big)\right]\times \quad (5.1)$$
$$\int d^2rd^2r'\,\frac{1}{2}\Big\{\sigma(\alpha r)+\sigma(\alpha r')-\sigma(\alpha|\vec r-\vec r\,'|)\Big\}\,\Psi_{V-A}^{\lambda_G}(\vec r,\alpha,M)\Psi_{V-A}^{\lambda_G*}(\vec r\,',\alpha,M)\,e^{i\vec q_\perp\cdot(\vec r-\vec r\,')}\,.$$

The principal difference of the inclusive gauge boson production from the diffractive one is in the typical size of the dipoles involved in the scattering. As is seen from e.g. Eqs. (2.13), (3.8), the diffractive scattering is dominated by large dipoles scattering at the hadronic scale, with the transverse size $r_p=R_{ij}\sim R_0$ (soft scattering), whereas the inclusive production cross section (5.1) is totally driven by small-size dipoles scattering with $r_p=\alpha r\ll R_0$ (hard scattering). Therefore, different parameterizations for the dipole cross sections must be used – in the diffractive case above we have adopted the KST parametrization for the dipole cross section (or the partial amplitude (3.12)) with s-dependent parameters introduced in Eq. (3.13) [13, 27], whereas in the inclusive production case the Bjorken x-dependent GBW parametrization Eq. (2.13) [32] is better justified:

$$\bar\sigma_0=23.03\,\mathrm{mb}\,,\quad R_0\equiv\bar R_0(x_2)=0.4\,\mathrm{fm}\times(x_2/x_0)^{0.144}\,,\quad x_0=3.04\times10^{-4}\,, \quad (5.2)$$

where $x_2=q^-/P_2^-$, with P_2 being the 4-momentum of the target proton.

In the leading regime of αr, $\alpha r'\ll R_0$.

$$\frac{1}{2}\Big\{\sigma(\alpha r)+\sigma(\alpha r')-\sigma(\alpha|\vec r-\vec r\,'|)\Big\}\simeq\frac{\alpha^2\bar\sigma_0}{\bar R_0^2(x_2)}\,(\vec r\cdot\vec r\,'), \quad (5.3)$$

so the inclusive gauge boson production cross section at forward rapidities ($x_1 \gg x_2$) reads,

$$\frac{d^4\sigma_{\lambda_G}(pp\to G^*X)}{d^2q_\perp\,dx_1} = \frac{1}{(2\pi)^2}\frac{\bar\sigma_0}{\bar R_0^2(x_2)}\sum_q\int_{x_1}^1 d\alpha\left[\rho_q\Big(\frac{x_1}{\alpha}\Big)+\rho_{\bar q}\Big(\frac{x_1}{\alpha}\Big)\right]\times \tag{5.4}$$
$$\int d^2r d^2r'\,(\vec r\cdot\vec r')\,\Psi^{\lambda_G}_{V-A}(\vec r,\alpha,M)\Psi^{\lambda_G*}_{V-A}(\vec r',\alpha,M)\,e^{i\vec q_\perp\cdot(\vec r-\vec r')}\,.$$

We observe that the integrals over α and $\vec r$, $\vec r\,'$ have the same form as in the diffractive cross section Eq. (4.5).

The M-dependence of the differential cross sections for di-lepton inclusive production via an intermediate photon γ^* or a gauge boson G^* can be presented similar to the diffractive case, as [28],

$$\frac{d\sigma_{\lambda_\gamma}(pp\to(\gamma^*\to l\bar l)X)}{d^2q_\perp dx_1\,dM^2} = \frac{\alpha_{em}}{3\pi M^2}\,\frac{d\sigma(pp\to\gamma^*X)}{d^2q_\perp dx_1}\,; \tag{5.5}$$
$$\frac{d\sigma(pp\to(G^*\to l\bar l,\,l\bar\nu_l)X)}{d^2q_\perp dx_1\,dM^2} = \mathrm{Br}(G\to l\bar l,\,l\nu_l)\,\rho_G(M)\,\frac{d\sigma(pp\to G^*X)}{d^2q_\perp dx_1}\,,$$

where the resonance mass distribution $\rho_G(M)$ is given by Eq. (3.3).

Eventually, we arrive at a simple form for the ratio of the diffractive and inclusive cross sections for di-lepton production,

$$\frac{d\sigma^{sd}_{\lambda_G}/d^2q_\perp\,dx_1\,dM^2}{d\sigma^{incl}_{\lambda_G}/d^2q_\perp dx_1\,dM^2} = \frac{a^2}{6\pi}\frac{\bar R_0^2(M_\perp^2/x_1s)}{B_{sd}(s)\,\bar\sigma_0}\frac{\sigma_0^2(s)}{R_0^4(s)}\,\frac{1}{A_2}\Big[\frac{2}{(A_2-4A_1)^2}+\frac{A_2^2}{(A_2^2-4A_3^2)^2}\Big] \tag{5.6}$$

where functions $A_{1,2,3}$ were defined in Eq. (4.6), and fraction x_2 is explicitly given in terms of other kinematic variables in Eq. (4.6).

It turns out that the ratio (5.6) does not depend either on the type of the intermediate boson, or on its helicity λ_G. To a good approximation, it is controlled mainly by soft interaction dynamics, in terms of the soft parameters only $\bar R_0$, R_0, $\bar\sigma_0$ and σ_0. A slow dependence of these parameters on the collision energy s, the hard scale M^2 and the boson transverse momentum $q_\perp$ completely determines such dependence of the diffractive-to-inclusive production ratio. A measurement of the M^2 (or $q_\perp$) dependence of this ratio would allow to probe the x-evolution of the saturation scale, as well as to constrain its energy dependence. Hence, such a quantity is a very useful probe for the underlined QCD diffractive mechanism and the saturation phenomenon, and will be quantified based on existing KST/GBW parameterizations in the next section.

VI. BREAKDOWN OF DIFFRACTIVE FACTORIZATION

It is instructive to trace the origin of QCD factorisation in inclusive processes within the dipole description. The $1/Q^2$ dependence of the DIS cross section at small x originates from two different sources. Most of the $\bar qq$ fluctuations of a virtual photon have a small size, $r^2\sim 1/Q^2$, except the endpoint (aligned jet) configurations with $\alpha\to 0,\ 1$. The latter have large hadronic size and cross section, but their weight is small $\sim 1/Q^2$. Thus, both contributions to the cross section behave as $1/Q^2$.

Similarly, in the Drell-Yan process of radiation of the heavy photon with fractional momentum x_1 the mean size of the artificial dipole [22] has small size $r \sim 1/(1-\alpha)Q$, except the endpoint configurations with $\alpha \to 1$. Like in DIS, α is not an observable, but is integrated from x_1 to 1 (see Eq. (5.1)). This similarity, which reflects the factorisation relation between the two processes, also demonstrates its limitations. At large $x_1 \to 1$ the inclusive Drell-Yan reaction is fully dominated by the soft component and factorisation breaks down.

For the diffractive channels the factorisation relation breaks down at any x_1. DIS diffraction is fully dominated by the soft dynamics, since the probability of endpoint configurations is still the same, $\propto 1/Q^2$, while the cross section is enhanced by a factor of Q^4 compared with the hard component [5]. However, the mechanism of Drell-Yan diffraction is quite different [15, 16], apparently breaking the factorisation relation. It comes from the hard-soft interference, which imitates a leading twist throughout the whole range of x_1. Again, like in inclusive process, the hard and soft (endpoint) components make comparable contributions to the diffractive Drell-Yan cross sections. Of course, this is true for other gauge bosons as well.

Although involvement of large distances in diffractive heavy boson production is in obvious contradiction with factorisation of hard and soft scales, an observable manifestation of that is not trivial. Indeed, the cross section of a hard process $q\bar{q} \to l\bar{l}$ with the sea quark density in the Pomeron measured in diffractive DIS, although it is a higher twist, imitates the leading twist scale dependence. Nevertheless, the predicted scale and energy dependences are quite different, as we demonstrate in the next Section VII. Notice that a much more pronounced breakdown of diffractive factorisation was previously found in Ref. [14] for the case when the hard scale is imposed by the mass of a heavy flavor.

VII. NUMERICAL RESULTS

We now turn to a discussion of the numerical results for the most important observables. First of all, we are interested in the di-lepton (*à la* Drell-Yan pair) production channel as the simplest one. Although quark production channel could also be of interest, this case will be considered elsewhere.

In Fig. 1 (for RHIC energy $\sqrt{s} = 500$ GeV) and Fig. 2 (for LHC energy $\sqrt{s} = 14$ TeV) we present the single diffractive cross sections for Z^0, γ^* (diffractive DY) and $W^\pm$ bosons production, differential in the di-lepton mass squared $d\sigma_{sd}/dM^2$ (left panels) and its longitudinal momentum fraction, $d\sigma_{sd}/dx_1$ (right panels). These plots do not reflect particular detector constraints – a thorough analysis including detector acceptances and cuts has to be done separately. The M^2 distributions here are integrated over the *ad hoc* interval of fractional boson momentum $0.3 < x_1 < 1$, corresponding to the forward rapidity region (at not extremely large masses). Then the mass distribution is integrated over the potentially interesting invariant mass interval $5 < M^2 < 10^5$ GeV^2, and can be easily converted into (pseudo)rapidity ones widely used in experimental studies, if necessary.

The M^2 distributions of the Z^0 and $W^\pm$ bosons clearly demonstrate their resonant behavior, and in the resonant region significantly exceed the corresponding diffractive Drell-Yan component; only for very low masses the γ^* contribution becomes important (left panels). For x_1 distribution, when integrated over low mass and resonant regions, diffractive W^+ and γ^* components become comparable to each other, both in shapes and values, whereas the W^- and, especially, Z-boson production cross section are noticeably lower (right panels). Quite naturally, the W^- cross section is (in analogy with the well-known inclusive $W^\pm$

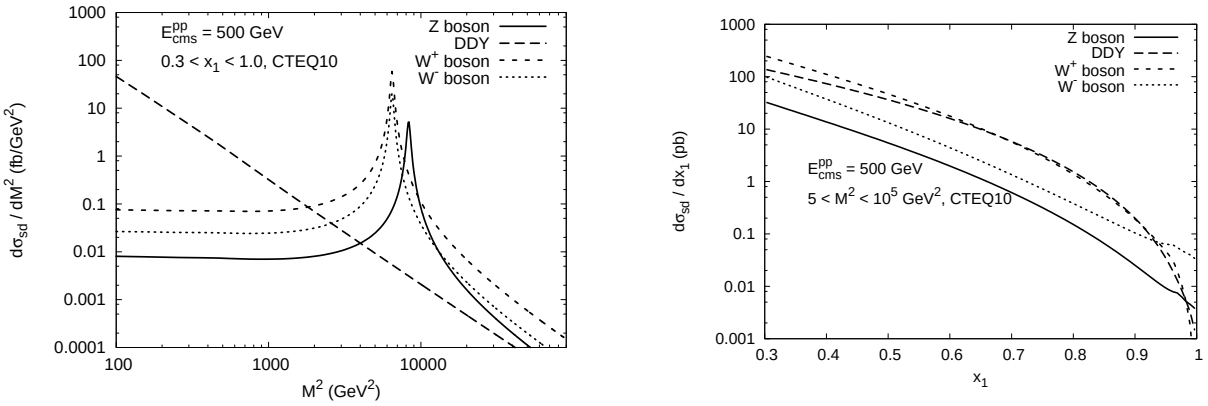

FIG. 1: Diffractive gauge boson production cross section as function of di-lepton invariant mass squared M^2 (left panel) and boson fractional light-cone momentum x_1 (right panel) in pp collisions at the RHIC energy $\sqrt{s} = 500$ GeV. Solid, long-dashed, dashed and dotted curves correspond to Z, γ^*, W^+ and W^- bosons, respectively. CTEQ10 PDF parametrization [34] is used here.

production) smaller than the W^+ one due to differences in valence u- and d-quark densities (dominating over sea quarks at large x_q) in the proton, the bosons couple to. So the precise measurement of differences in forward diffractive W^+ and W^- rates would allow to constrain quark content of the proton at large $x_q \equiv x_1/\alpha$. In Fig. 1 and 2, and in all calculation below we have used the most recent CTEQ10 valence/sea quark PDFs parametrization [34], if not declared otherwise.

In Fig. 3 we show the ratio of the longitudinal (L) to transverse (T) gauge boson polarization contributions to the diffractive production cross section. This ratio is presented differentially as function of lepton-pair invariant mass squared $(\sigma^L_{sd}/dM^2)/(\sigma^T_{sd}/dM^2)$ (left panel) and gauge boson fractional momentum $(\sigma^L_{sd}/dx_1)/(\sigma^T_{sd}/dx_1)$ (right panel). We see that the diffractive gauge bosons production process is always dominated by radiation of transversely polarized lepton pairs. The ratio σ_L/σ_T only slightly depends on M^2 and even less on pp c.m. energy $\sqrt{s}$, so it can be considered as energy independent (which, in fact, can be already seen from approximate formulae (4.9) and (4.10)). The longitudinal bosons polarization roughly amounts to 10 % at $x_1 \sim 0.5$ and then steeply falls down at large $x_1 \to 1$

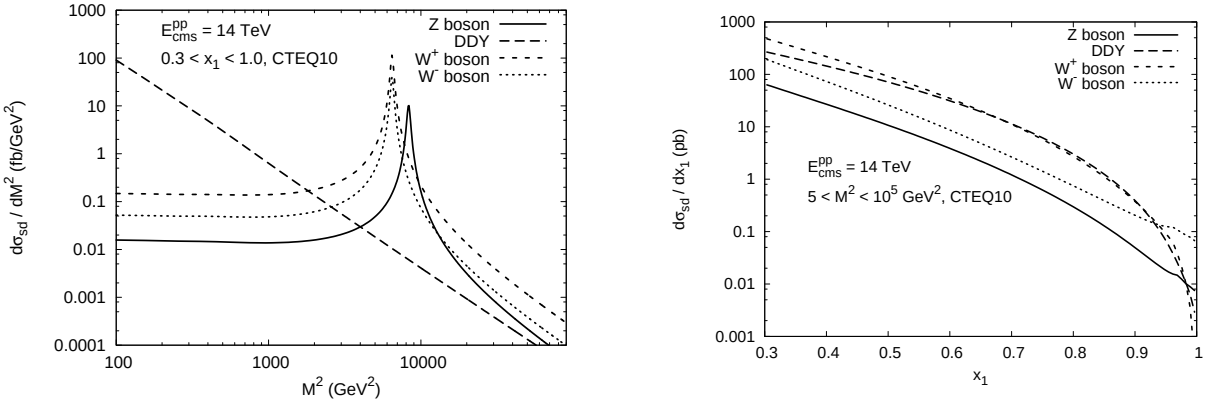

FIG. 2: The same as in Fig. 1, but for the LHC energy $\sqrt{s} = 14$ TeV.

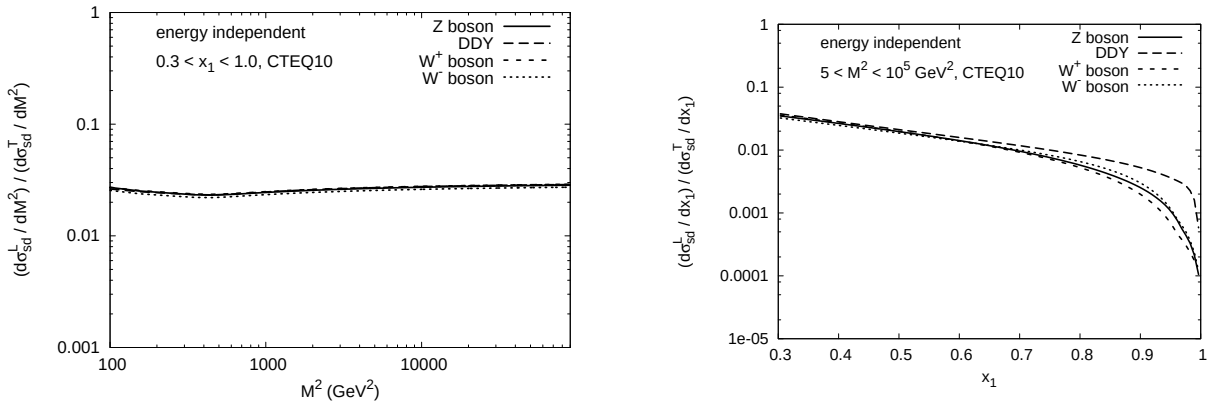

FIG. 3: The ratio of the cross sections of longitudinally (L) to transversely (T) polarized gauge bosons, as function of the di-lepton invariant mass squared M^2 (left panel), and boson fractional light-cone momentum x_1 (right panel). Solid, long-dashed, dashed and dotted curves correspond to Z, γ^*, W^+ and W^- bosons, respectively. CTEQ10 PDF parametrization [34] is used here. The ratio depends on pp c.m. energy only slightly, by a few percents (*cf.* Ref. [16]) over a vast multi-TeV interval, so we neglect it here.

asymptotically approaching relativistic (massless) bosons case given, due to the gauge invariance, by the transverse polarisation only. Such a behavior turns out to be the same as in the inclusive Drell-Yan process [15]. At smaller $x_1 \lesssim 0.6$ this ratio becomes the same for different bosons, whereas at large $x_1 \to 1$ the relative contribution of the longitudinally polarized photon dominates in corresponding ratios for other bosons.

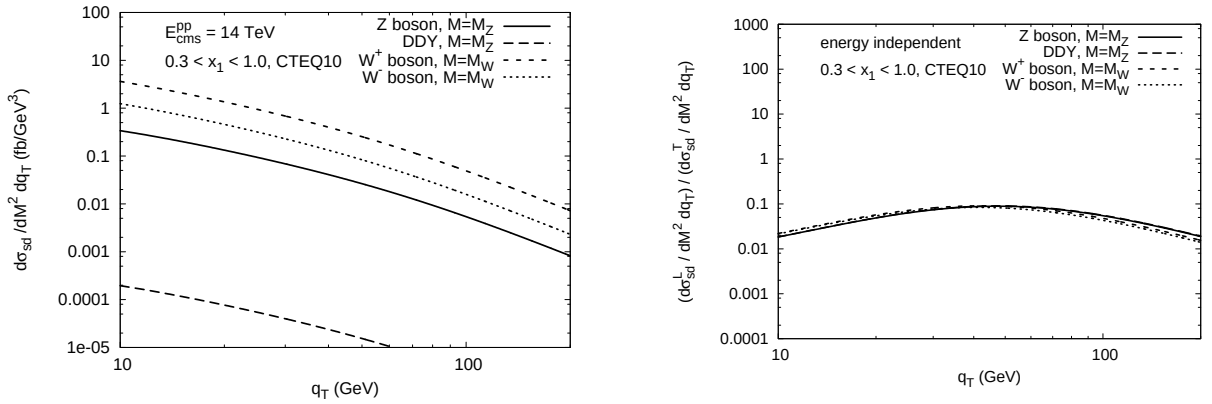

FIG. 4: The di-lepton transverse momentum $q_\perp$ distribution of the doubly-differential diffractive cross section at the LHC energy $\sqrt{s} = 14$ TeV at fixed di-lepton invariant mass is shown in the left panel. The longitudinal-to-transverse gauge bosons polarisations ratio as a function of the di-lepton $q_\perp$ is shown in the right panel. In both panels, the invariant mass is fixed as $M = M_Z$ in the Z^0, γ^* production case and as $M = M_W$ in the $W^\pm$ production case. CTEQ10 PDF parametrization [34] is used here.

From the phenomenological point of view, the distribution of the forward diffractive

cross section in the di-lepton transverse momentum $q_\perp$ could also be of major importance[4]. In Fig. 4 (left panel) we show the di-lepton transverse momentum $q_\perp$ distribution of the doubly-differential diffractive cross section at the LHC energy $\sqrt{s} = 14$ TeV at the di-lepton invariant mass, fixed at a corresponding resonance value – the Z or W mass. The shapes turned out to be smooth and the same for different gauge bosons, and are different mostly in normalisation. In Fig. 4 (right panel) we show the $q_\perp$ dependence of the σ^L/σ^T ratio in the resonances. We notice that the ratio does not strongly vary for different bosons. It is peaked at about the half of the resonance mass, and uniformly decreases to smaller/larger $q_\perp$ values.

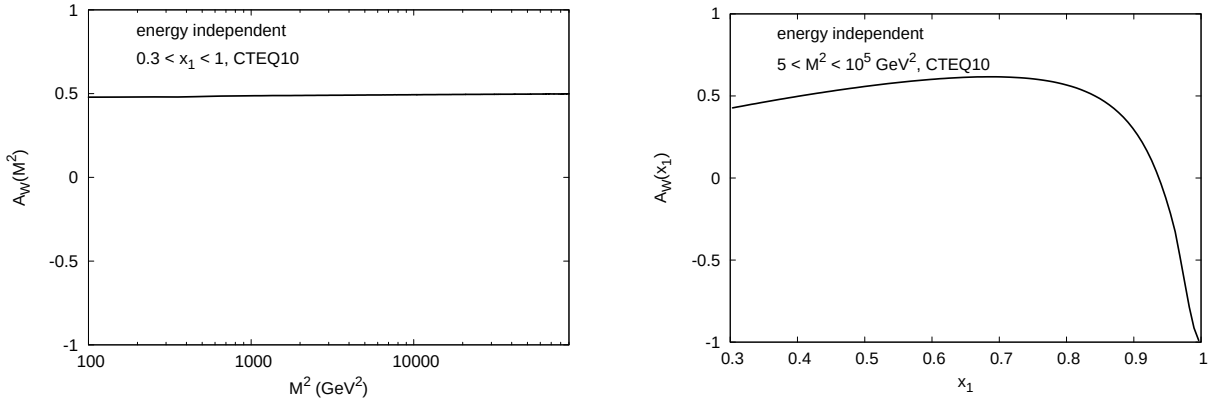

FIG. 5: Charge asymmetry in the single diffractive W^+ and W^- cross sections as a function of M^2, at fixed $x_1 = 0.5$ (left panel), and x_1, at fixed $M^2 = M_W^2$ (right panel). Solid lines correspond to the LHC energy $\sqrt{s} = 14$ TeV, dished lines – to the RHIC energy $\sqrt{s} = 500$ GeV.

As one of the important observables, sensitive to the difference between u- and d-quark PDFs, the $W^\pm$ charge asymmetry A_W is shown in Fig. 5 differentially as a function of the di-lepton invariant mass squared M^2 and integrated over $0.3 < x_1 < 1.0$ interval (left panel)

$$A_W(M^2) = \frac{d\sigma_{sd}^{W^+}/dM^2 - d\sigma_{sd}^{W^-}/dM^2}{d\sigma_{sd}^{W^+}/dM^2 + d\sigma_{sd}^{W^-}/dM^2}\,, \tag{7.1}$$

and as a function of the boson momentum fraction x_1 and integrated over $5 < M^2 < 10^5$ GeV^2 interval (right panel)

$$A_W(x_1) = \frac{d\sigma_{sd}^{W^+}/dx_1 - d\sigma_{sd}^{W^-}/dx_1}{d\sigma_{sd}^{W^+}/dx_1 + d\sigma_{sd}^{W^-}/dx_1}\,. \tag{7.2}$$

The ratio turns out to be independent on both the hard scale M^2 and the c.m. energy $\sqrt{s}$. One concludes that, due to different x-shapes of valence u, d quark PDFs, at smaller $x_1 \lesssim 0.9$ the diffractive W^+ bosons' rate dominates over W^- one. However, at large $x_1 \to 1$ the W^- boson cross section becomes increasingly important and strongly dominates over the W^+ one.

[4] Authors are indebted to Torbjörn Sjöstrand for pointing out this point.

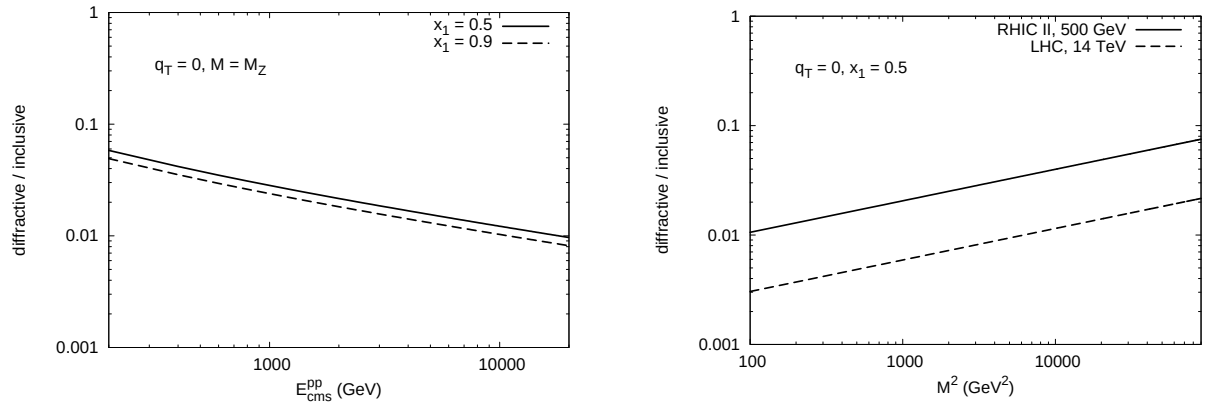

FIG. 6: The diffractive-to-inclusive ratio of the gauge bosons production cross sections in pp collisions derived in Eq. (5.6) as a function of the c.m. energy $\sqrt{s}$ (left panel) and the di-lepton invariant mass M^2 (right panel). It does not depend on the type of the gauge boson and quark PDFs.

An important feature of the diffractive-to-inclusive Abelian radiation cross sections ratio

$$R(M^2, x_1) = \frac{d\sigma_{sd}/dx_1 dM^2}{d\sigma_{incl}/dx_1 dM^2}\,, \tag{7.3}$$

which makes these predictions different from ones obtained in traditional diffractive QCD factorisation-based approaches (see e.g. Refs. [11, 12]), is their unusual energy and scale dependence demonstrated in Fig. 6. Notice that we stick to the case of small boson transverse momenta, $q_\perp \ll M$, where the main bulk of diffractive signals comes from. The analytic formula for this ratio was derived above and is shown by Eq. (5.6), which deminstrates that the ratio is independent of the type of the gauge boson, its polarisation, or quark PDFs. In this respect, it is the most convenient and model independent observable, which is sensitive only to the structure of the universal elastic dipole amplitude (or the dipole cross section), and can be used as an important probe for the QCD diffractive mechanism for forward diffractive reactions, essentially driven by the soft interaction dynamics. We see from Fig. 6 that the $\sigma_{sd}/\sigma_{incl}$ ratio decreases with energy, but increases with the hard scale, thus behaves opposite to what is expected in the diffractive factorisation-based approaches. Therefore, measurements of the single diffractive gauge boson production cross section, at least, at two different energies would provide important information about the interplay between soft and hard interactions in QCD, and its role in formation of diffractive excitations and color screening effects.

Finally, in Fig. 7 we present the diffractive-to-inclusive cross sections ratio as a function of the boson fractional momentum x_1 at RHIC ($\sqrt{s} = 500$ GeV) and at LHC ($\sqrt{s} = 14$ TeV) energies (left panel). In the right panel, we compare this ratio calculated at the Tevatron energy ($\sqrt{s} = 1.96$ TeV) with the recent measurements of diffractive W and Z production performed by the CDF collaboration [9]. The data show the x_1-integrated ratio of diffractive to inclusive cross sections. Due to the weak x_1-dependence of this ratio (left panel) with a good accuracy the integrated values are numerically close to the ratio of differential cross sections given by Eq. (7.3). We see that the results of our calculations with Eq. (5.6) at $x_1 = 0,5$ agree well with the data. This agreement is another confirmation of correctness of the absorption effects included into the parametrization of the dipole cross section (3.12).

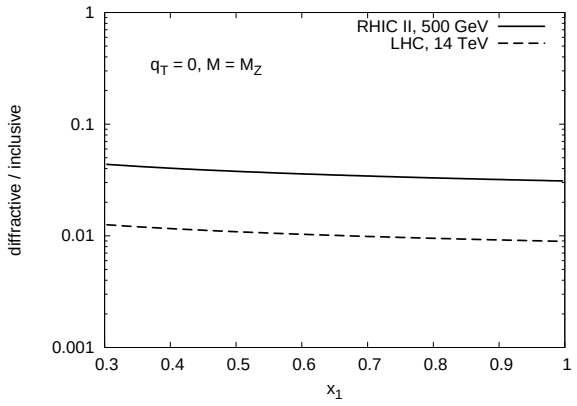

FIG. 7: The diffractive-to-inclusive ratio as function of the boson fractional momentum x_1.

VIII. LINK TO THE REGGE PHENOMENOLOGY AND DATA

The process $pp \to Xp$ at large Feynman $x_F \to 1$ of the recoil proton, or small

$$\xi = 1 - x_F = \frac{M_X^2}{s} \to 0, \tag{8.1}$$

is described by triple Regge graphs as is illustrated in Fig. 8. Here we also included pro-

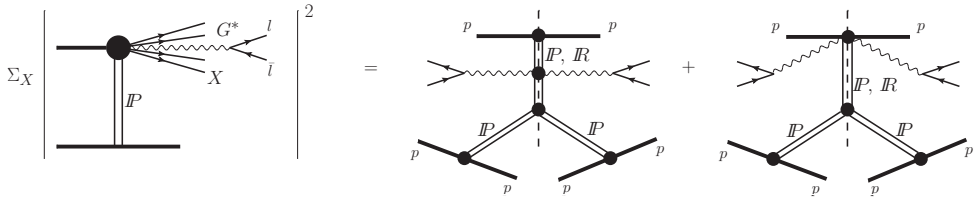

FIG. 8: Triple-Regge description of the process $pp \to Xp$, where the diffractively produced state X contains a gauge boson decaying to a lepton pair (see text).

duction radiation of a gauge boson. The incoming proton can diffractively dissociate either due to excitation of the quark skeleton, what corresponds to the triple-Regge graph $I\!P I\!P I\!R$, or via gluon radiation corresponding to the triple-Pomeron term, $I\!P I\!P I\!P$. So far our calculations did not specify which of these terms is related to radiation of the gauge boson. At first glance we considered only the valence quark Fock component of the proton. In such a case only the $I\!P I\!P I\!R$ graph would contribute, what corresponds to the configuration in the projectile proton, when the main momentum fraction is carried by two quarks, while the third one has a tiny fractional momentum $x \sim m_{q,T}^2/M_X^2$, where $m_{q,T}^2 = m_q^2 + p_\perp^2$ is the transverse quark mass squared. The gauge boson can be radiated either from the quark with minimal fractional momentum (the first term in the r.h.s. of Fig. 8), or from one of the two high fractional momentum quarks (the second term in Fig. 8).

The triple-Pomeron term corresponds to diffractive excitation via gluon radiation. This process corresponds to the projectile configuration in which the fractional momenta of the valence quarks are of the same order, while a gluon (or several of them) carry a tiny fraction. In this case the gauge boson can be radiated either by a sea quark (the first term in Fig. 8), or by one of the valence quarks (the second term in Fig. 8).

Gluons in the light-cone wave function of the proton should also be considered as spectator partons, and the large distance R_{ij} in Eq. (4.1) in this case is the quark-gluon separation. In fact, our calculation did include such configurations. Indeed, data on diffraction show that diffractive gluon radiation is quite weak (well known smallness of the triple-Pomeron coupling), and this can be explained assuming that gluons in the proton are located within small "spots" around the valence quarks with radius $r_0 \sim 0.3\,\mathrm{fm}$ [13, 37–39]. Therefore, the large distance between one valence quark and a satellite-gluon of another quark is approximately equal (with 10% accuracy) to the quark-quark separation. Since a valence quark together with co-moving gluons is a color triplet, in our calculations the interaction amplitude of such an effective ("constituent") quark with the target is a coherent sum of the quark-target and gluon-target interaction amplitudes.

Thus, our calculations effectively cover the gluon radiation, so the triple-Pomeron term is included. This is important because this term dominates the diffractive cross section [40]. So we can compare with available data from the CDF experiment [9] on W and Z diffractive production depicted in Fig. 9.

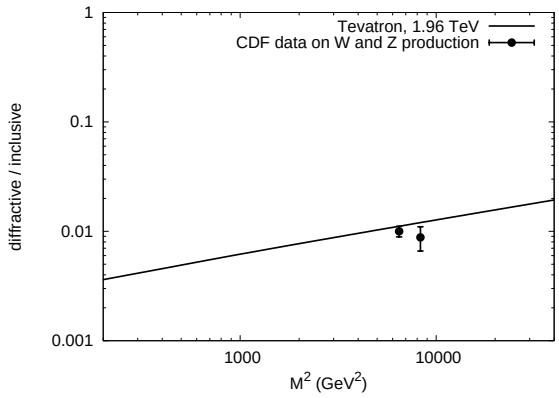

FIG. 9: The diffractive-to-inclusive ratio as function of the invariant mass squared of the produced dilepton. The CDF data for W and Z production were taken at the Tevatron energy ($\sqrt{s} = 1.96$ TeV). The first CDF data point corresponds to the W production, $M^2 = M_W^2$, the second – to the Z production, $M^2 = M_Z^2$.

However, in order to compare our results with CDF data, we have to introduce in our calculations the accessible experimental cuts, namely, $0.03 < \xi < 0.1$ [9]. Since our diffractive cross section formulae are differential in M^2, not in M_X^2, and experimental cuts on y-rapidity distribution of a produced gauge boson are unavailable at the moment, a direct implementation of the ξ cuts into our formalism cannot be performed immediately.

As a way out of this problem, at small $\xi \to 0$ one can instead write the single diffractive cross section in the phenomenological triple-Regge form [40],

$$-\frac{d\sigma_{sd}^{pp}}{d\xi\, dp_T^2} = \sqrt{\frac{s_1}{s}}\,\frac{G_{I\!P I\!P I\!R}(0)}{\xi^{3/2}}\, e^{-B_{I\!P I\!P I\!R} p_T^2} + \frac{G_{3I\!P}(0)}{\xi}\, e^{-B_{3I\!P}^{pp} p_T^2}\,, \tag{8.2}$$

where $s_1 = 1\,\mathrm{GeV}^2$; $B_{I\!P I\!P i} = R_{I\!P I\!P i}^2 - 2\alpha'_{I\!P}\,\ln\xi$; $i = I\!P, I\!R$; and $\alpha'_{I\!P} \approx 0.25\mathrm{GeV}^{-2}$ is the slopes of the Pomeron trajectory. Then an effect of the experimental cuts on ξ in the phenomenological cross section (8.2) and in our diffractive cross section calculated above (3.6) should roughly be the same.

Since the data show no substantial rise of the diffractive cross section with energy [41, 42], which is apparently caused by strong absorptive corrections, we incorporate this fact fixing the effective Pomeron intercept at $\alpha_{I\!P}(0) = 1$. This also allows us to use the results of the comprehensive triple-Regge analysis of data performed in Ref. [40], which led to the following values of the parameters: $G_{3I\!P}(0) = G_{I\!P I\!P I\!R}(0) = 3.2$ mb/GeV^2; $R^2_{3I\!P} = 4.2\,\mathrm{GeV}^{-2}$; $R^2_{I\!P I\!P I\!R} = 1.7\,\mathrm{GeV}^{-2}$.

Now we are in a position to evaluate the suppression factor δ caused by experimental cut on ξ, by taking the ratio

$$\delta = \frac{\int dp_T^2 \int_{0.03}^{0.1} d\xi\, d\sigma/dp_T^2 d\xi}{\int dp_T^2 \int_{\xi_{min}}^{\xi_{max}} d\xi\, d\sigma/dp_T^2 d\xi} \tag{8.3}$$

Here $\xi_{min} = M^2_{X,min}/s$, where $M_{X,min} \simeq M_Z$ is the minimal produced diffractive mass containing a heavy gauge boson. The value of δ in Ref. (8.3) is essentially determined by the experimental cuts on ξ and is not sensitive to the upper limit ξ_{max} in denominator, so we fix it at a realistic value[5]: $\xi_{max} \sim 0.3$. Then Eq. (8.3) leads to $\delta \simeq 0.2$, the factor reducing the diffractive gauge bosons production cross section calculated above. Our result plotted in Fig. 9 demonstrates a good agreement with the CDF data on single diffractive W and Z production [9].

IX. CONCLUSIONS

The diffractive radiation of Abelian fields, γ, Z^0, $W^\pm$, expose unusual features, which make it very different from diffraction in DIS, and lead to a dramatic breakdown of QCD factorisation in diffraction.

The first, rather obvious source for violation of diffractive factorisation is related to absorptive corrections (called sometimes survival probability of large rapidity gaps). The absorptive corrections affect differently the diagonal and off-diagonal terms in the hadronic current [35], leading to an unavoidable breakdown of QCD factorisation in processes with off-diagonal contributions only. Namely, the absorptive corrections suppress the off-diagonal diffraction much stronger than the diagonal channels. In the diffractive Abelian radiation in hadron-hadron collisions a new state, i.e. the gauge boson decaying into the heavy lepton pair, is produced, hence, the whole process is of entirely off-diagonal nature, whereas in the diffractive DIS contains both diagonal and off-diagonal contributions [4]. This is the first reason why QCD factorisation is broken in the diffractive gauge bosons production processes.

The second, more sophisticated reason to contradict diffractive factorisation is specific for Abelian radiation, namely, a quark cannot radiate in the forward direction (zero momentum transfer), where diffractive cross sections usually have a maximum. Forward diffraction becomes possible due to intrinsic transverse motion of quarks inside the proton.

Third, the mechanism of Abelian radiation in the forward direction in pp collisions is related to participation of the spectator partons in the proton. Namely, the perturbative

[5] The estimate for $\xi_{max} \sim 0.3$ corresponds to the limiting case when one of the constituent quarks in a target (anti)proton looses almost all its energy into a hard radiation of a gluon in the t-channel. The second and all subsequent t-channel gluon exchanges collectively screen the color charge taken away from the target by the first gluon and transfer much smaller fraction of initial target momentum to projectile quarks as has been recently advocated in Refs. [43, 44].

QCD interaction of a projectile quark is responsible for the hard process of a heavy boson radiation, while a soft interaction with the projectile spectator partons provides color neutralization [43, 44], which is required for a diffractive (Pomeron exchange) process. Such an interplay of hard and soft dynamics is also specific for the process under consideration, which makes it different from the diffractive DIS, dominated exclusively by soft interactions, and which also results in breakdown of diffractive factorisation.

The diffractive (Ingelman-Schlein) QCD factorisation breaking manifests itself in specific features of diffractive observables like a significant damping of the single diffractive gauge bosons production cross section at high $\sqrt{s}$ compared to the inclusive production case. This is rather unusual, since a diffractive cross section, which is proportional to the dipole cross section squared, could be expected to rise with energy steeper than the total inclusive cross section, like it occurs in the diffractive DIS process. At the same time, the ratio of the single diffractive to inclusive production cross sections rises with the hard scale, M^2. This is also in variance with diffraction in DIS associated with the soft interactions.

In this paper, we have presented the differential distributions (in transverse momentum, invariant mass and longitudinal momentum fraction) of the diffractive γ^*, Z^0 and $W^\pm$ bosons production at RHIC (500 GeV) and LHC (14 TeV) energies, as well as the ratio of the boson longitudinal to transverse polarisation contributions. We have also calculated the charge $W^\pm$ asymmetry, relevant for upcoming measurements at the LHC. The ratio diffractive to inclusive gauge bosons production cross sections does not depend on a particular type of the gauge boson, its polarisation state and quark PDFs, and depends only on properties of the universal dipole cross section and sensitive to the saturation scale at small x. Finally, our prediction for this ratio is numerically consistent with the one measured for diffractive W and Z production at the Tevatron.

The theoretical uncertainties of our calculations come mainly from poorly known quark PDFs (or the proton structure function $F_2(x_q)$ in diffractive DY) at large quark fractions $x_q \to 1$. This issue has been discussed in our previous analysis of the DDY process in Ref. [16], where a strong sensitivity of the x_1 dependence to a particular F_2 parametrization has been pointed out. The same situation extends to the more general case of diffractive Abelian radiation considered in this paper. This tells us again that measurements of forward diffractive gauge bosons production would be extremely important or even crucial for settling further more stringent constraints on the quark content of the proton.

Acknowledgments

Useful discussions and helpful correspondence with Gunnar Ingelman, Valery Khoze, Eugene Levin, Amir Rezaeian, Christophe Royon, Torbjörn Sjöstrand and Antoni Szczurek are gratefully acknowledged. This study was partially supported by Fondecyt (Chile) grant 1090291, and by Conicyt-DFG grant No. 084-2009.

---

[1] R. J. Glauber, Phys. Rev. 100, 242 (1955).

[2] E. Feinberg and I. Ya. Pomeranchuk, Nuovo. Cimento. Suppl. 3 (1956) 652.

[3] M. L. Good and W. D. Walker, Phys. Rev. 120 (1960) 1857.

[4] B. Z. Kopeliovich, I. K. Potashnikova, I. Schmidt, Braz. J. Phys. **37**, 473-483 (2007). [arXiv:hep-ph/0604097 [hep-ph]].

[5] B. Z. Kopeliovich and B. Povh, Z. Phys. A **356**, 467 (1997) [nucl-th/9607035].

[6] B. Z. Kopeliovich, L. I. Lapidus and A. B. Zamolodchikov, JETP Lett. **33**, 595 (1981) [Pisma Zh. Eksp. Teor. Fiz. **33**, 612 (1981)].
[7] G. Ingelman, P. E. Schlein, Phys. Lett. **B152** 256 (1985).
[8] F. Abe *et al.* [CDF Collaboration], Phys. Rev. Lett. **78**, 2698 (1997) [hep-ex/9703010].
[9] T. Aaltonen *et al.* [CDF Collaboration], Phys. Rev. D **82**, 112004 (2010) [arXiv:1007.5048 [hep-ex]].
[10] K. A. Goulianos, hep-ph/9708217.
[11] G. Kubasiak and A. Szczurek, Phys. Rev. D **84**, 014005 (2011) [arXiv:1103.6230 [hep-ph]].
[12] M. B. Gay Ducati, M. M. Machado and M. V. T. Machado, Phys. Rev. D **75**, 114013 (2007) [hep-ph/0703315].
[13] B. Z. Kopeliovich, A. Schäfer and A. V. Tarasov, Phys. Rev. **D62**, 054022 (2000) [arXiv:hep-ph/9908245].
[14] B. Z. Kopeliovich, I. K. Potashnikova, I. Schmidt and A. V. Tarasov, Phys. Rev. D **76**, 034019 (2007) [hep-ph/0702106 [HEP-PH]].
[15] B. Z. Kopeliovich, I. K. Potashnikova, I. Schmidt, A. V. Tarasov, Phys. Rev. **D74**, 114024 (2006).
[16] R. S. Pasechnik and B. Z. Kopeliovich, arXiv:1109.6690 [hep-ph]; Eur. Phys. J. C **71**, 1827 (2011) [arXiv:1109.6695 [hep-ph]].
[17] K. Golec-Biernat and A. Luszczak, Phys. Rev. D **81**, 014009 (2010).
[18] K. Golec-Biernat, C. Royon, L. Schoeffel and R. Staszewski, arXiv:1110.1825 [hep-ph].
[19] K. Nakamura *et al.* [Particle Data Group Collaboration], J. Phys. G G **37**, 075021 (2010).
[20] H. L. Lai, M. Guzzi, J. Huston, Z. Li, P. M. Nadolsky, J. Pumplin and C. P. Yuan, Phys. Rev. D **82**, 074024 (2010).
[21] V. I. Kuksa and R. S. Pasechnik, Int. J. Mod. Phys. A **23**, 4125 (2008); Phys. Atom. Nucl. **73**, 1622 (2010); Mod. Phys. Lett. A **26**, 1075 (2011);
[22] B. Z. Kopeliovich, proc. of the workshop Hirschegg 95: Dynamical Properties of Hadrons in Nuclear Matter, Hirschegg January 16-21, 1995, ed. by H. Feldmeyer and W. Nörenberg, Darmstadt, 1995, p. 102 (hep-ph/9609385);
[23] S. J. Brodsky, A. Hebecker, and E. Quack, Phys. Rev. **D55** (1997) 2584.
[24] B. Z. Kopeliovich, A. V. Tarasov and A. Schafer, Phys. Rev. C **59**, 1609 (1999) [hep-ph/9808378].
[25] B. Z. Kopeliovich, H. J. Pirner, A. H. Rezaeian and I. Schmidt, Phys. Rev. D **77**, 034011 (2008) [arXiv:0711.3010 [hep-ph]].
[26] B. Z. Kopeliovich, I. K. Potashnikova, I. Schmidt and J. Soffer, Phys. Rev. D **78**, 014031 (2008) [arXiv:0805.4534 [hep-ph]].
[27] B. Z. Kopeliovich, A. H. Rezaeian, I. Schmidt, Phys. Rev. **D78**, 114009 (2008) [arXiv:0809.4327 [hep-ph]].
[28] B. Z. Kopeliovich, J. Raufeisen, A. V. Tarasov, Phys. Lett. **B503**, 91-98 (2001). [hep-ph/0012035].
[29] R M. Barnett *et al.*, Rev. Mod. Phys. 68, 611 (1996).
[30] G. T. Garvey and J. -C. Peng, Prog. Part. Nucl. Phys. **47**, 203 (2001).
[31] S. Amendolia *et al.*, Nucl. Phys. **B277**, 186 (1986).
[32] K. J. Golec-Biernat, M. Wusthoff, Phys. Rev. **D59**, 014017 (1998). [hep-ph/9807513].
[33] J. Bartels, K. J. Golec-Biernat and H. Kowalski, Phys. Rev. D **66** (2002) 014001.
[34] H. L. Lai, M. Guzzi, J. Huston, Z. Li, P. M. Nadolsky, J. Pumplin and C. P. Yuan, Phys. Rev. D **82**, 074024 (2010) [arXiv:1007.2241 [hep-ph]].

[35] B. Z. Kopeliovich, I. K. Potashnikova, I. Schmidt, M. Siddikov, Phys. Rev. **C84**, 024608 (2011) [arXiv:1105.1711 [hep-ph]].
[36] J. C. Collins, D. E. Soper and G. F. Sterman, Adv. Ser. Direct. High Energy Phys. **5**, 1 (1988) [hep-ph/0409313].
[37] T. Schafer, E.V. Shuryak, Rev. Mod. Phys. **70**, 323 (1998).
[38] E. Shuryak and I. Zahed, Phys. Rev. D69 (2004) 014011.
[39] B. Z. Kopeliovich, I. K. Potashnikova, B. Povh and I. Schmidt, Phys. Rev. D **76** (2007) 094020 [arXiv:0708.3636 [hep-ph]].
[40] Yu.M. Kazarinov, B.Z. Kopeliovich, L.I. Lapidus and I.K. Potashnikova, JETP **70** (1976) 1152.
[41] K.Goulianos, J. Montanha, Phys. Rev. **D59**, 114017 (1999)
[42] S. Erhan and P.E. Schlein, Phys. Lett. **B427** (1998) 389.
[43] R. Pasechnik, R. Enberg and G. Ingelman, Phys. Rev. D **82**, 054036 (2010) [arXiv:1005.3399 [hep-ph]].
[44] R. Pasechnik, R. Enberg and G. Ingelman, Phys. Lett. B **695**, 189 (2011) [arXiv:1004.2912 [hep-ph]].